Dynamic Modeling of Magnetorheological Damper Behaviors

SHUQI GUO,[1,*] SHAOPU YANG[1] AND CUNZHI PAN[2]

[1]*Department of Mechanics and Engineering Science, Shijiazhuang Railway Institute, Shijiazhuang, Hebei 050043, China*

[2]*School of Mechanical, Electronic and Control Engineering of Beijing Jiaotong University, Beijing 100044, China*

ABSTRACT: Based on theoretical analysis and experiments, this article proposes a new model for a magnetorheological (MR) damper. The proposed model with a smooth and concise form can interpret the bi-viscous and hysteretic behaviors of the MR damper very well. The parameters in the model have definite physical meanings. The bi-viscous and hysteretic behaviors can be characterized by two parameters θ_0 and A_3. The proposed model makes it convenient to study the effects of the bi-viscous and hysteretic behaviors on the performance of a system with a MR damper. As one application of the model, a vibration isolation system with a MR damper is investigated, and the effects of bi-viscous and hysteretic behaviors on system performances are studied by numerical methods and theoretical analysis.

Key Words: MR damper, modeling, bi-viscous behavior, hysteretic behavior.

INTRODUCTION

MAGNETO-RHEOLOGICAL (MR) fluid is one kind of smart material that has the unique ability to change its properties when a magnetic field is applied (Carlson et al., 1995). A MR damper is a familiar and important device among numerous applications of MR fluids (Jolly et al., 2000; Gandhi et al., 2001; Yang, 2001; Choi et al., 2002; Choi and Han, 2003). MR dampers exhibit bi-viscous and hysteretic behaviors when subjected to sinusoidal load. The system with a MR device exhibits strong nonlinear dynamical behavior. Modeling of a MR device under certain loading conditions is one of the key challenges in analyzing the essential nonlinear dynamical behavior of the entire system. Many models are put forward to characterize the dynamic behaviors of MR dampers, which include the Bingham model (Stanway et al., 1987), the nonlinear bi-viscous model (Stanway et al., 1997), the bi-viscous hysteresis model (Pang et al.; Wereley et al., 1998), the phenomenological Bouc-Wen model (Spencer et al., 1997), the polynomial model (Choi et al., 2001), the modified Bingham hysteresis model (Yang et al., 2005), and a unified model for ER and MR vibration damper (Sims et al., 2004).

All of these models can capture the post-yield behavior of MR dampers. The Bingham model is the simplest model. The nonlinear bi-viscous model can capture the bi-viscous behavior. In bi-viscous hysteresis model, the bi-viscous and hysteretic behaviors are described by a six-section piecewise function with three parameters. The phenomenological Bouc-Wen model takes a 14-parameter first-order nonlinear differential equation, which is frequently used to analyze the nonlinear hysteretic behaviors. The polynomial model is expressed as a polynomial function of piston velocity, which can describe the hysteresis behavior and can be easily integrated with a control system. The modified Bingham hysteresis model can capture the hysteretic behavior. The unified model is an application of the nonlinear bi-viscous model integrated with the parameter identification technique.

Two of the above mentioned models could be able to describe not only the bi-viscous behavior but also the hysteretic behavior of MR dampers. The first one is the phenomenological Bouc-Wen model, and the second one is the bi-viscous hysteresis model. However, because of the complicated forms, the two models are inconvenient to be used in control and analysis of dynamical performance of an MR system, such as nonlinear frequency response functions.

A new model with a smooth and concise form is proposed in this article. The proposed model can describe the bi-viscous and hysteretic behaviors of the MR damper very well. Compared with the phenomenological Bouc-Wen model and the bi-viscous hysteresis model, the smooth and concise form of the proposed model make it convenient to investigate the dynamical performance of the systems with MR dampers numerically and theoretically. In addition, the parameters in

*Author to whom correspondence should be addressed.
E-mail: shuqig@yahoo.com.cn

1045-389X/06/01 0003–12 $10.00/0 DOI: 10.1177/1045389X06055860

proposed model have definite physical meanings. The model parameters θ_0 and A_3 can characterize the bi-viscous and hysteretic behaviors of MR dampers respectively. Then it can be used to investigate the effects of the bi-viscous and hysteretic behaviors on system performances. The two mentioned parameters are insensitive to the coil currents, which is convenient to control.

The article is arranged as following. The experiment scheme is introduced in the next section. In the section 'The Proposed Model and Theoretical Analysis', the proposed model and its theoretical analysis are submitted. The authors submit the proposed model and discuss its relation with the Bingham model at first. Then it is clarified that the proposed model could characterize the hysteretic behavior of MR dampers, and an equivalent force–velocity form of the model is given. At the end of the section, the physical meaning of the model parameters is discussed. The section 'Numeric Simulations and Some Discussions' presents numerical simulations and some discussions on the model. As an application of the proposed model, a vibration isolation system with an MR damper is studied numerically and theoretically in the section 'An Application: A Vibration Isolation System with MR Damper'. The conclusions are drawn in the last section.

THE EXPERIMENT SCHEME AND TEST RESULTS

The schematic illustration of the tested MR damper is shown in Figure 1. The MR damper is designed by the Shijiazhuang Railway Institute (Haijun et al., 2002). The performance of the MR damper is tested with MTS system, as shown in Figure 2. A displacement sensor and a force sensor, controlled by Teststar US, measure piston displacement and damper force respectively. Velocity is derived from numerical differentiation of the displacement.

A series of tests are conducted to measure the response of the damper under various sinusoidal loading

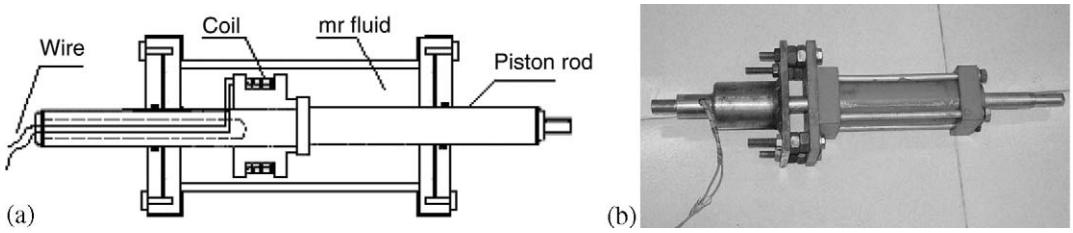

Figure 1. *Schematic of the tested damper: (a) structure and (b) digital photo.*

Figure 2. *Experimental setup of MR damper in the MTS810-23.*

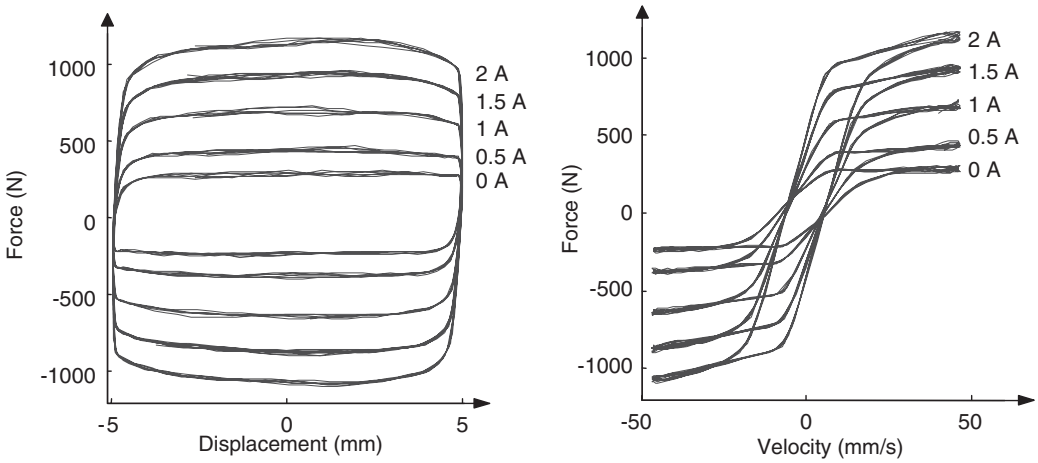

Figure 3. *A group of data under 0.5 cm 1.5 Hz sinusoidal displacement excitation. Left: Force–displacement and Right: Force–velocity.*

conditions. The performance test consists of frequency sweep held at constant displacement input, which are 0.5, 1.0, and 2.0 cm. The input electric current applied to the MR damper is maintained at a constant level of 0, 0.5, 1.0, 1.5, and 2.0 A. One group of experimental results is presented in Figure 3. More experimental results may be seen in Appendix A. One can find that the MR damper exhibits strong nonlinear bi-viscous and hysteretic behaviors in Figure 3.

THE PROPOSED MODEL AND THEORETICAL ANALYSIS

The Proposed Model

The proposed model for the MR damper is shown in Equation (1).

$$F_{\mathrm{md}} = A_1 \tanh\left(A_3\left(\dot{x} + \frac{V_0}{X_0}x\right)\right) + A_2\left(\dot{x} + \frac{V_0}{X_0}x\right), \quad (1)$$

where F_{md} is MR damper force, x and $\dot{x}$ are displacement and velocity of the damper piston respectively. A_1 is dynamic yield force of MR fluid, A_2 and A_3 are parameters related to post-yield and pre-yield viscous damping coefficients respectively, V_0 and X_0 denote the absolute value of hysteretic critical velocity $\dot{x}_0$ and hysteretic critical displacement x_0 respectively. $\dot{x}_0$ and x_0 are defined as the piston velocity and displacement when MR damper force F_{md} is zero, respectively. Apparently, one has

$$\dot{x}_0 = \pm V_0, \quad (2)$$

$$x_0 = \mp X_0, \quad (3)$$

where the $+V_0$ and the $-X_0$ hold when the piston moves along the positive x direction, and vice versa. When exciting displacement x is sinusoidal, one could assume

$$x = a\sin\theta, \quad (4)$$

$$\dot{x} = a\omega\cos\theta, \quad (5)$$

$$\theta = \omega t + \varphi, \quad (6)$$

where f is frequency and $\omega = 2\pi f$, a the amplitude of x, φ initial phase angle and θ is phase angle.

From Equations (2)–(5), one obtains

$$V_0^2 + \omega^2 X_0^2 = a^2\omega^2. \quad (7)$$

Then one could assume

$$V_0 = a\omega\sin\theta_0, \quad (8)$$

$$X_0 = a\cos\theta_0, \quad (9)$$

$$0 \le \theta_0 < \frac{\pi}{2}, \quad (10)$$

From Equations (8) and (9), θ_0 could be rewritten as:

$$\theta_0 = \arctan\frac{V_0}{\omega X_0}, \quad (11)$$

where θ_0 is a model parameter that denotes phase lag. Substituting Equations (8) and (9) into Equation (1) yields Equation (12), which is equivalent with Equation (1).

$$F_{\mathrm{md}} = A_1\tanh(A_3(\dot{x} + \omega x\tan\theta_0)) + A_2(\dot{x} + \omega x\tan\theta_0). \quad (12)$$

When $\theta_0 = 0$ and $A_3 = \infty$, one may get Equation (13), which is the well-known Bingham model.

$$F_{\mathrm{md}} = A_1\,\mathrm{sgn}\,\dot{x} + A_2 x. \quad (13)$$

From the analysis in following subsections, one will find that $\theta_0 = 0$ when the hysteretic behavior of MR dampers is neglected; $A_3 = \infty$ if the pre-yield region of MR dampers is neglected. When piston velocity is constant, $\omega = 0$. Substituting $\omega = 0$ and $A_3 = \infty$ into Equation (12), one may obtain the Bingham model again. It may be seen from Equations (8) and (9) that $V_0 = 0$ when $\theta_0 = 0$ or $\omega = 0$. Substituting $V_0 = 0$ and $A_3 = \infty$ into Equation (1), one may reduce Equation (1) as the equation for the Bingham model. It may be seen clearly that the Bingham model is only a special case of our proposed model, when the hysteresis and pre-yield region in damper are neglected.

Parameter θ_0 and the Hysteretic Behavior of MR Damper

From Equations (4)–(6) and (10), Equation (12) may be formulated as

$$\begin{aligned} F_{\mathrm{md}} &= A_1 \tanh(A_3(\dot{x} + \omega x \tan\theta_0)) + A_2(\dot{x} + \omega x \tan\theta_0) \\ &= A_1 \tanh\left(\frac{A_3}{\cos\theta_0}(\dot{x}\cos\theta_0 + \omega x \sin\theta_0)\right) \\ &\quad + \frac{A_2}{\cos\theta_0}(\dot{x}\cos\theta_0 + \omega x \sin\theta_0) \\ &= A_1 \tanh\left(\frac{A_3 a\omega}{\cos\theta_0}\cos(\theta - \theta_0)\right) + \frac{A_2 a\omega}{\cos\theta_0}\cos(\theta - \theta_0). \end{aligned}$$

This leads to Equation (14), which is equivalent to Equation (1) for sinusoidal excitations.

$$F_{\mathrm{md}} = A_1 \tanh\left(\frac{A_3 a\omega}{\cos\theta_0}\cos(\theta - \theta_0)\right) + \frac{A_2 a\omega}{\cos\theta_0}\cos(\theta - \theta_0). \tag{14}$$

Taking a look at the force–velocity relationship in Figures 3 and 4, one knows that the signs of damper force F_{md} and velocity are approximately identical. However, the variations of the sign of damper force are always later than that of velocity, which is an important character of hysteresis loop. In Equation (14), the variations of the sign of F_{md} are later than that of $\cos\theta$; the sign of $\cos\theta$ is identical with the sign of damper piston velocity $\dot{x}$. Apparently model parameter θ_0 is related to the hysteretic loop in Figures 3 and 4.

The Equivalent Force–Velocity Model

One could deduce Equation (15) from Equations (4) and (5).

$$x = \begin{cases} \dfrac{1}{\omega}\sqrt{a^2\omega^2 - \dot{x}^2}, & \dfrac{\mathrm{d}\dot{x}}{\mathrm{d}t} > 0 \\ -\dfrac{1}{\omega}\sqrt{a^2\omega^2 - \dot{x}^2}, & \dfrac{\mathrm{d}\dot{x}}{\mathrm{d}t} < 0 \end{cases} \tag{15}$$

Substituting Equation (15) into Equation (12) yields

$$F_{\mathrm{md}} = \begin{cases} A_1 \tan\left(A_3\left(\dot{x} - \dfrac{V_0}{\omega X_0}\sqrt{a^2\omega^2 - \dot{x}^2}\right)\right) \\ \quad + A_2\left(\dot{x} - \dfrac{V_0}{\omega X_0}\sqrt{a^2\omega^2 - \dot{x}^2}\right), & \dfrac{\mathrm{d}\dot{x}}{\mathrm{d}t} > 0 \\ A_1 \tan\left(A_3\left(\dot{x} + \dfrac{V_0}{\omega X_0}\sqrt{a^2\omega^2 - \dot{x}^2}\right)\right) \\ \quad + A_2\left(\dot{x} + \dfrac{V_0}{\omega X_0}\sqrt{a^2\omega^2 - \dot{x}^2}\right), & \dfrac{\mathrm{d}\dot{x}}{\mathrm{d}t} < 0. \end{cases} \tag{16}$$

Then Equations (1) and (12) are equivalent to Equation (16) for sinusoidal excitations. From previous discussions, one knows that the proposed model has three equivalent forms, Equations (12), (14) and (16). The three mentioned equations describe force–velocity–displacement, force–phase, and force–velocity relations respectively. A typical curve of Equation (16) is shown in Figure 4. Figure 4 further illustrates that the proposed model may describe the hysteretic and bi-viscous behavior of MR dampers quite well.

Figure 5 shows a typical curve of the bi-viscous hysteresis model (Pang et al.). This model could be

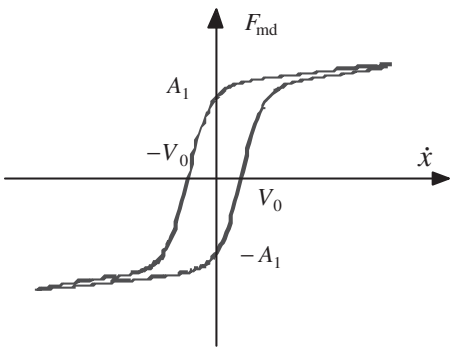

Figure 4. *A typical curve of the proposed model.*

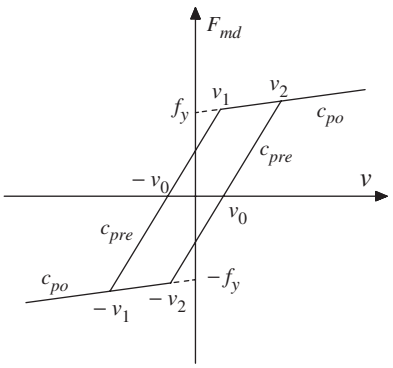

Figure 5. *The bi-viscous hysteresis model.*

described by Equation (17).

$$F_{\mathrm{md}} = \begin{cases} c_{\mathrm{po}} v - f_{\mathrm{y}} & v \le -v_1 \quad \dot{v} > 0 \\ c_{\mathrm{pre}}(v - v_0) & -v_1 \le v \le v_2 \quad \dot{v} > 0 \\ c_{\mathrm{po}} v + f_{\mathrm{y}} & v_2 \le v \quad \dot{v} > 0 \\ c_{\mathrm{po}} v + f_{\mathrm{y}} & v_1 \le v \quad \dot{v} < 0 \\ c_{\mathrm{pre}}(v + v_0) & -v_2 \le v \le v_1 \quad \dot{v} < 0 \\ c_{\mathrm{po}} v + f_{\mathrm{y}} & v \le -v_2 \quad \dot{v} < 0 \end{cases} \tag{17}$$

where v is piston velocity, c_{pre} pre-yield viscous damping coefficients, c_{po} post-yield viscous damping coefficients, and f_{y} yield force.

The Physical Meanings of the Model Parameters

In order to explain the physical meanings of the model parameters A_1, A_2 and A_3, the Bingham model is rewritten as

$$F_{\mathrm{md}} = c_1 \operatorname{sgn} \dot{x} + c_2 \dot{x}, \tag{18}$$

where c_1 is the dynamic yield force, which is a function of applied current, c_2 is the viscous damping coefficient.

From previous discussion, it is known that parameter A_1 is the dynamic yield force, then $A_1 = c_1$. From Equation (14) and the fact that MR fluids mainly work on post-yield region, it is clear Equation (19) holds approximately.

$$F_{\max} = A_1 + \frac{A_2 V_{\max}}{\cos\theta_0}. \tag{19}$$

When $F_{\max}$ denotes the maximum damper force, $V_{\max} = a\omega$ is the maximum piston velocity. Then A_2 from the above equation can be solved.

$$A_2 = \frac{F_{\max} - A_1}{V_{\max}} \cos\theta_0. \tag{20}$$

Considering Equation (19), it is easy to know

$$F_{\max} = c_1 + c_2 V_{\max}. \tag{21}$$

Then, with the relation $A_1 = c_1$ and Equation (21), one obtains

$$\frac{F_{\max} - A_1}{V_{\max}} = c_2. \tag{22}$$

Substituting Equation (22) into Equation (20) yields

$$A_2 = c_2 \cos\theta_0. \tag{23}$$

It can be seen from Equation (23) that the parameter A_2 is a measurement of viscous damping coefficient c_2, which also presents the physical meaning of the parameter A_2.

In subsection 'The Proposed Model', the authors claimed that the parameter A_3 is a measurement of pre-yield viscous damping of MR dampers. Now the meaning of A_3 can be explained more accurately. First a notation σ is defined.

$$\sigma = \dot{x} + \frac{V_0}{X_0} x. \tag{24}$$

From Equation (17) and the relations $f_{\mathrm{y}} = A_1$, $v = \dot{x}$, one can obtain

$$F_{\mathrm{md}} = A_1, \quad \text{when } \dot{x} = \frac{A_1}{c_{\mathrm{pre}}} + V_0. \tag{25}$$

A reasonable assumption is that Equation (25) is also right for the proposed model. Considering Equation (24) and substituting Equation (25) into Equation (1), one obtains

$$1 - \frac{A_2}{A_1}\sigma = \tanh(A_3\sigma).$$

Considering Equation (15), one can solve A_3 from the above equation.

$$A_3 = \frac{\operatorname{atanh}(1 - (A_2/A_1)\sigma)}{\sigma}, \tag{26}$$

where

$$\sigma = \frac{A_1}{c_{\mathrm{pre}}} + V_0 - V_0\sqrt{1 - \tan^2\theta_0 \frac{A_1}{V_0 c_{\mathrm{pre}}}\left(2 + \frac{A_1}{V_0 c_{\mathrm{pre}}}\right)}.$$

When θ_0 is small, Equation (27) holds approximately.

$$A_3 = \frac{\operatorname{atanh}\left(1 - (A_2/c_{\mathrm{pre}})\left(\begin{matrix}1 + \tan^2\theta_0 \\ +(1/2)\tan^2\theta_0 (A_1/V_0 c_{\mathrm{pre}})\end{matrix}\right)\right)}{(A_1/c_{\mathrm{pre}})(1 + \tan^2\theta_0 + (1/2)\tan^2\theta_0 (A_1/V_0 c_{\mathrm{pre}}))}. \tag{27}$$

Equations (26) and (27) clarifies the relation between the parameters A_3 and c_{pre}. If the hysteresis behavior is neglected, i.e. $\theta_0 = 0$, the relations (26) and (27) are reduced as Equation (28).

$$A_3 = \frac{c_{\mathrm{pre}} \operatorname{atanh}\left(1 - (A_2/c_{\mathrm{pre}})\right)}{A_1}. \tag{28}$$

Figure 6 is the schematic of the proposed model. The hysteretic character of damping force can be described by phase lag; and the phase lag can be described by the linear combination of piston velocity $\dot{x}$ and displacement x, i.e., $\dot{x} + (V_0/X_0)x$, which is embodied in subsection 'Parameter θ_0 and the Hysteretic Behavior of MR Damper'.

The proposed model has a simple and smooth expression, which is an extended Bingham model by using a shape function *tanh* and the term $\dot{x} + (V_0/X_0)x$ instead of $\dot{x}$. Apparently it is smoother and more accurate than the bi-viscous hysteresis model, which is verified in the next section. The second term in the proposed model, $A_2(\dot{x} + (V_0/X_0)x)$, is a linear combination of piston velocity $\dot{x}$ and displacement x. The first

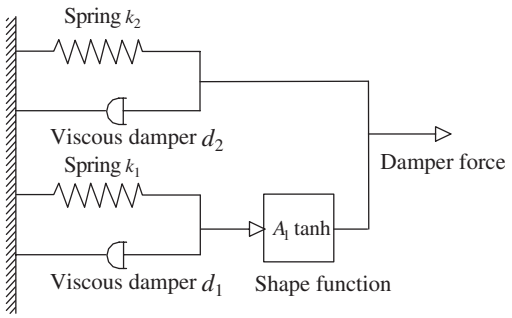

Figure 6. *The schematic of the proposed model, where* $k_1 = A_3V_0/X_0$, $k_2 = A_2V_0/X_0$, $d_1 = A_3$, $d_2 = A_2$.

part of this term is $A_2\dot{x}$, which is the characteristic of the linear viscous damping of Newtonian fluids. The second part of the term is $A_2(V_0/X_0)x$, which is the characteristic of linear elastomers. It is a well-known fact that MR fluids exposed to an external magnet field consist mainly of two parts, i.e., the carrier liquid and the chain-like structure. So the structure of the proposed model is consistent with the fact.

NUMERIC SIMULATIONS AND SOME DISCUSSIONS

Figure 7 compares the simulation results of the Bingham model and the proposed model in excitation of 1 Hz frequency, 1 cm amplitude and 2 A electrical current. It can be seen clearly from Figure 7 that the Bingham model cannot describe the bi-viscous and hysteretic behaviors and the proposed model simulates the test data quite well. Figure 8 compares the simulation results of the bi-viscous hysteresis model in excitation of 1.5 Hz frequency, 5 mm amplitude and 2 A electrical current. It shows that the proposed model simulates the test data much better than that of the bi-viscous hysteresis model.

The value of A_1, A_2, A_3, X_0, V_0 are identified by least square method, which can be done by Matlab function *lsqcurvefit*.

From the force–velocity curves in Figure 3 and Appendix A, it can be seen that V_0 is constant for definite amplitude a and angular frequency ω. And, V_0 is also constant in bi-viscous hysteresis model (Stanway et al., 1997). From Equation (8), it is known that θ_0 is constant for definite a and angular frequency ω. That is to say, θ_0 is insensitive to the change of electric currents in coil. Table 1 presents the values of θ_0 for different amplitudes and frequencies when currents are 0, 0.5, 1, 1.5, and 2 A. Apparently the values of θ_0 near a constant for different electrical currents.

Figure 9 shows the values of parameter A_3 with different electrical currents in coil. One could find that the values of A_3 are also insensitive to the change of electrical currents in coil.

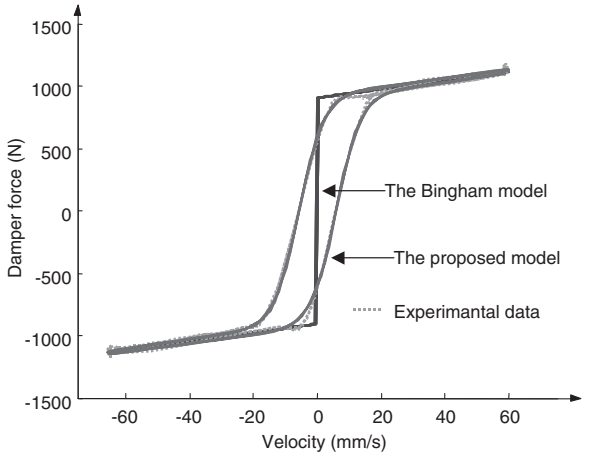

Figure 7. *Simulation in excitation of 1 Hz and 1 cm.*

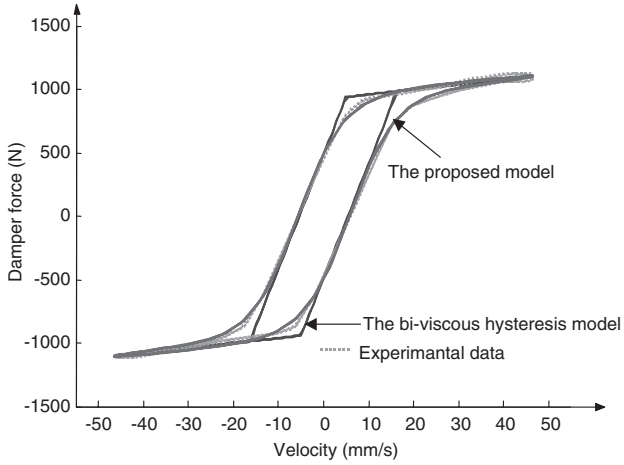

Figure 8. *Simulation in 1.5 Hz and 5 mm excitation.*

Table 1. The value of θ_0 ***for different electrical currents.***

	0.5 Hz 1 cm	1 Hz 1 cm	0.5 Hz 5 mm	1 Hz 5 mm	2 Hz 2 mm	3 Hz 2 mm
2 A	0.09	0.08	0.12	0.11	0.19	0.21
1.5 A	0.08	0.07	0.12	0.11	0.18	0.21
1 A	0.07	0.07	0.11	0.10	0.17	0.21
0.5 A	0.07	0.07	0.14	0.11	0.19	0.25
0 A	0.09	0.12	0.16	0.13	0.22	0.19
Average value	0.08	0.08	0.13	0.11	0.19	0.21

AN APPLICATION: A VIBRATION ISOLATION SYSTEM WITH MR DAMPER

The motion equation of the vibration isolation system shown in Figure 10 is

$$m\ddot{x} + kx + F_{\mathrm{md}} = p_0 \sin \omega t \tag{29}$$

where x is the displacement of the mass, m the mass, k the spring stiffness, $p_0 \sin \omega t$ the load excitation, and

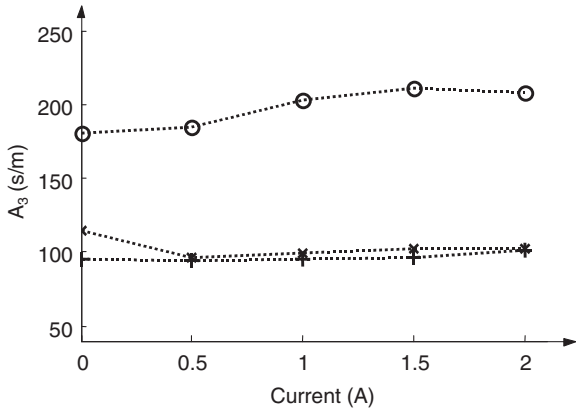

Figure 9. *The values of A_3. o: 1 Hz 5 mm, x: 1 Hz 10 mm, +: 1.5 Hz 5 mm.*

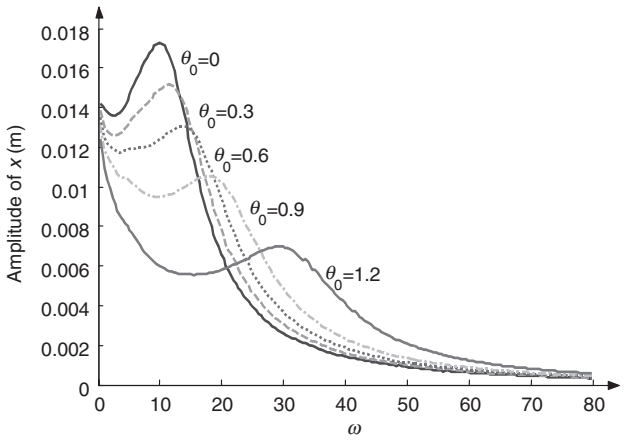

Figure 11. *The effect of the parameter θ_0 when $A_3 = 140$.*

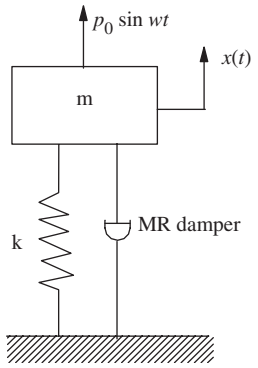

Figure 10. *A vibration isolation system with MR damper.*

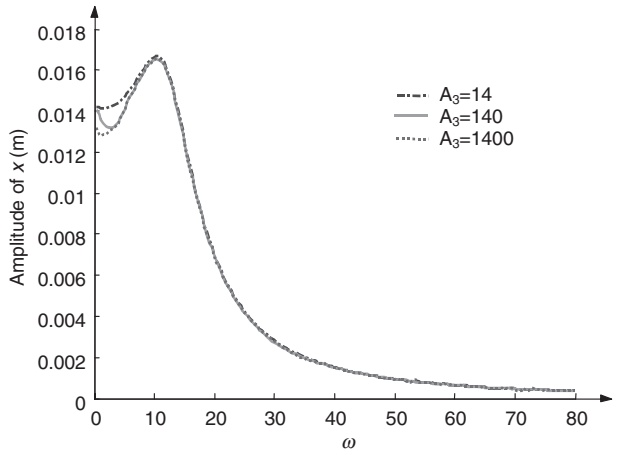

Figure 12. *The effect of the parameter A_3 when $\theta_0 = 0.1$.*

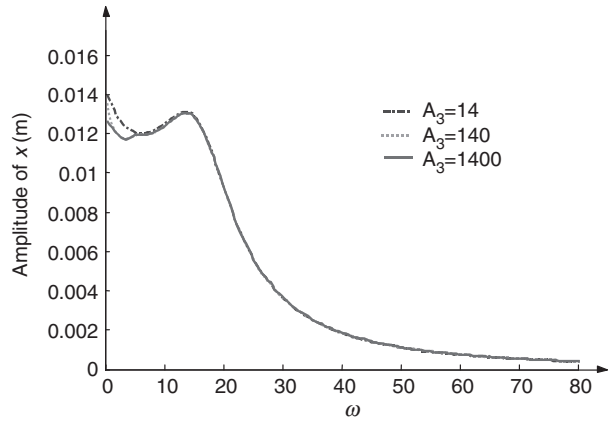

Figure 13. *The effect of the parameter A_3 when $\theta_0 = 0.6$.*

F_{md} the damping force. Substituting Equation (1) into Equation (29) yields

$$m\ddot{x} + \left(k + \frac{V_0}{X_0}A_2\right)x + A_2\dot{x} + A_1 \tanh\left(A_3\left(\dot{x} + \frac{V_0}{X_0}x\right)\right) = p_0 \sin \omega t. \quad (30)$$

Substituting Equation (11) into Equation (30), we have

$$m\ddot{x} + (k + A_2\omega \tan\theta_0)x + A_2\dot{x} + A_1 \tanh(A_3(\dot{x} + \omega x \tan\theta_0)) = p_0 \sin \omega t. \quad (31)$$

Now the authors investigate the harmonic response and the effects of model parameters on the response. It is known from previous sections that θ_0 and A_3 may characterize the hysteretic and the bi-viscous behavior of the MR damper respectively. Then one can investigate the effect of these behaviors on the vibration isolation system. Figures 11–13 show the numerical simulation results. The parameter values for numerical integrations are $A_1 = 900\,\text{N}$, $A_2 = 40{,}000\,\text{N/(m/s)}$, $p_0 = 9000\,\text{N}$, $k = 64{,}000\pi^2$, $m = 4000\,\text{kg}$, $\omega \in [0.3, 80]$, and the time span for numerical integration of 100 cycles, i.e., $100\omega/(2\pi)$.

Figure 11 illustrates the effect of the parameter θ_0 on the resonance frequency and the amplitude of the displacement of Equation (31) with $A_3 = 140\,\text{s/m}$. One can find that resonance frequency increases and the

amplitude of x decreases with increasing of θ_0 when excitation frequency is below the natural frequency of the system i.e., 2π rad/s. The amplitude of x increases with the increasing of θ_0 when excitation frequency is above the natural frequency. Figures 12 and 13 illustrate the effect of the parameter A_3 on the amplitude of x with $\theta_0 = 0.1$ and $\theta_0 = 0.6$, respectively. It is found that A_3 has a little impact on the amplitude of x, especially when excitation frequency is greater than the resonance frequency. The amplitude decreases with the increasing of A_3.

Let δ be the displacement amplitude of Equation (31). The amplitude–frequency equation is shown in Equation (32), which is obtained in Appendix B. It is an approximate solution.

$$\begin{aligned}&\left(-m\omega^2\delta + k\delta + A_2\delta\omega\tan\theta_0 + A_1\tanh(A_3\delta\omega\tan\theta_0)\right)^2\pi^2 \\ &\quad + \left(A_1\cos\theta_0 g\left(\frac{A_3\delta\omega}{\cos\theta_0}\right) + A_2\delta\omega\pi\right)^2 = p_0^2\pi^2 \end{aligned} \tag{32}$$

where $g(A_3\delta\omega/\cos\theta_0)$ is a function of the variable $(A_3\delta\omega/\cos\theta_0)$. The function $g(\cdot)$ is defined as

$$g(y) = \frac{-4\,\text{Elliptic K}\left(\sqrt{-y^2}\right) + \text{Elliptic E}\left(\sqrt{-y^2}\right)}{y}, \tag{33}$$

where EllipticK$(\cdot)$ and EllipticE$(\cdot)$ are the first and the second kind complete elliptic integrals, respectively.

The comparison between the theoretical and numerical simulations of Equation (31) is illustrated in Figure 14. The dotted lines in Figure 14 are theoretical results. The solid lines are numerical simulation results when $A_3 = 140$ s/m. Other parameters in numerical simulations keep unchanged as in previous section.

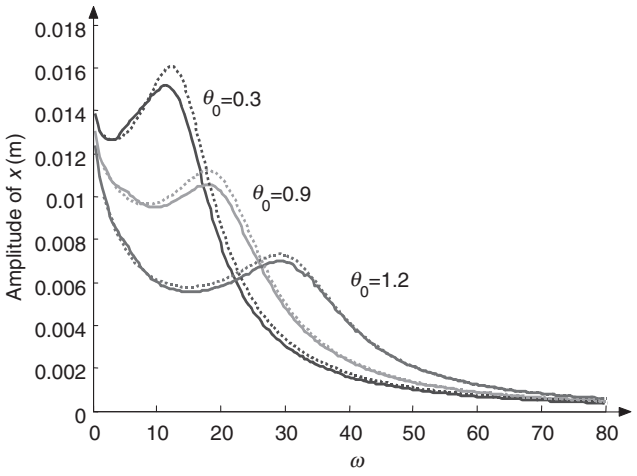

Figure 14. *The comparison between the theoretical solution and the numerical simulations. A3 = 140; — The numerical simulations, ... The theoretical results.*

The theoretical solutions agree with the numerical simulations quite well.

CONCLUSIONS

1. The proposed model with a smooth and concise form may describe bi-viscous and hysteretic behaviors of MR dampers very well. All the model parameters have definite physical meaning. The smooth and concise form of the model makes it easy to investigate the effects of bi-viscous and hysteretic behaviors on MR system performances.
2. The model parameters θ_0 and A_3 characterize the hysteretic and the bi-viscous behaviors of MR dampers respectively. The Bingham model is only a special case of the proposed model when the hysteresis and the pre-yield region of MR dampers are neglected. Numeric simulation indicates that the accuracy of the proposed model is higher than the Bingham model and the bi-viscous hysteresis model.
3. Parameter θ_0 can capture the hysteresis information of MR dampers, as shown in Equations (8), (9) and (14). Parameter A_3 can capture the bi-viscosity information of MR dampers, as shown in Equation (28). Both of the two parameters θ_0 and A_3 are insensitive to the coil currents, which is a good quality for control.
4. The proposed model has three equivalent forms, Equations (12), (14), and (16). The three equations may describe force–velocity–displacement, force–phase, and force–velocity relations respectively.
5. As an application, a vibration isolation system with MR damper is analyzed to show the effect of the bi-viscous and hysteretic behaviors on system performance. The numerical simulation shows that resonance frequency will increase with increasing of θ_0, which means that the width of the hysteresis loop increases; the displacement amplitudes will decrease or increase with the parameter θ_0 when excitation frequency is less or greater than the natural frequency of the isolation system respectively. The model parameter A_3 slightly influences the displacement amplitude especially when the excitation frequency is above resonance frequency.
6. A theoretical solution of the vibration isolation system is obtained, which may predict the response amplitude approximately.

ACKNOWLEDGMENTS

This study is supported in part by the National Science Foundation of China (NSFC) under the grant number 10472073, 10172060 and Science Foundation of Hebei under grant number E2005000507.

APPENDIX A

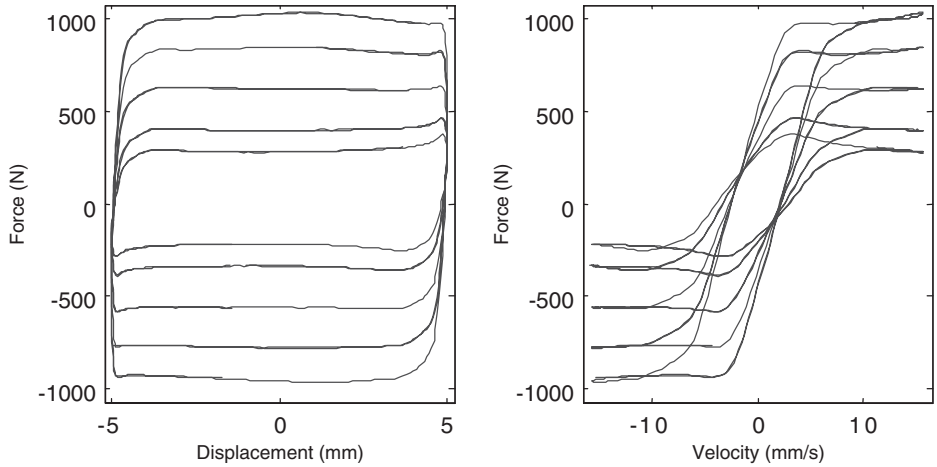

Figure A1. *The test data in excitation of 0.5 Hz and 5 mm.*

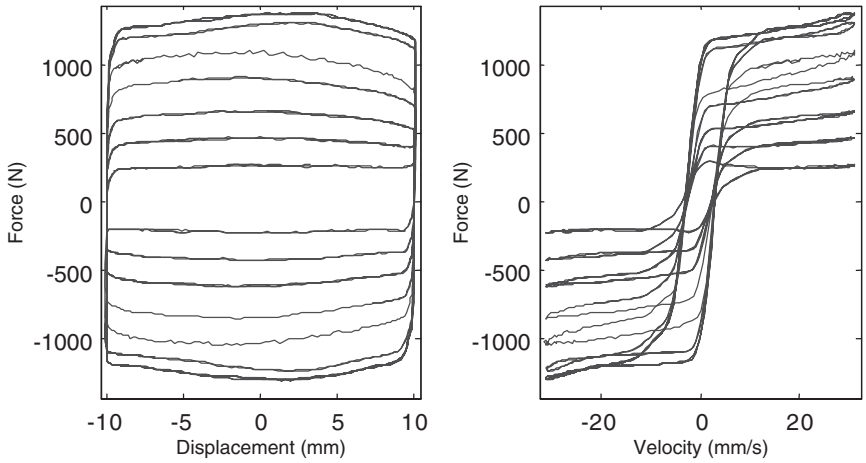

Figure A2. *The test data in excitation of 0.5 Hz and 10 mm.*

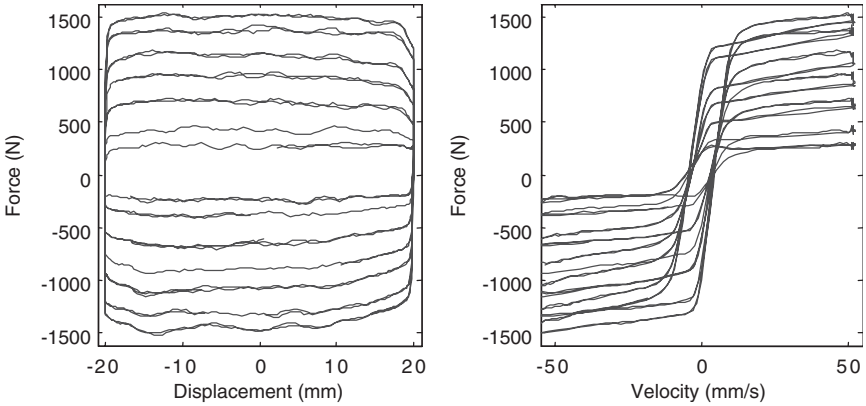

Figure A3. *The test data in excitation of 0.5 Hz and 20 mm.*

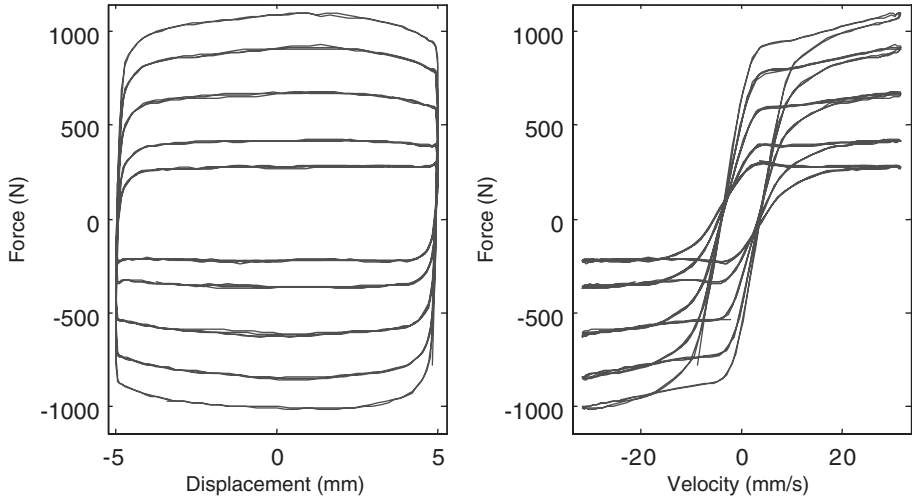

Figure A4. *The test data in excitation of 1 Hz and 5 mm.*

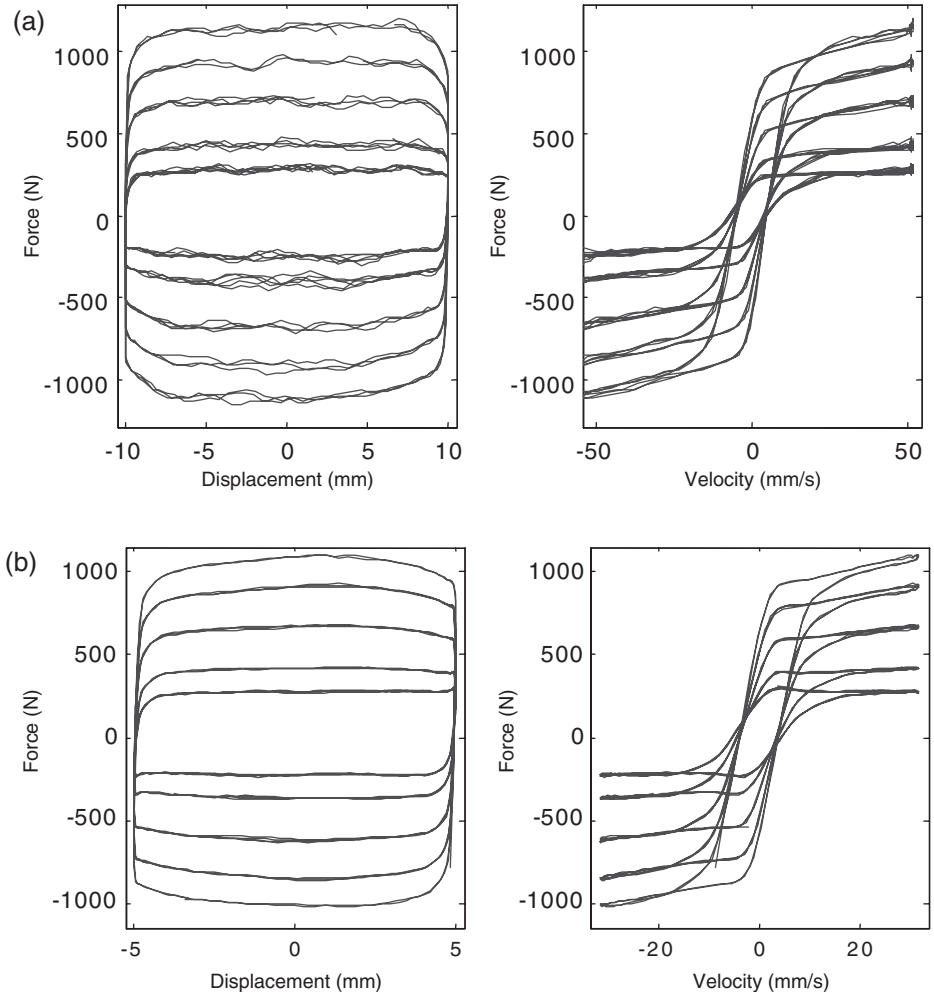

Figure A5. *The test data in excitation of (a) 1 Hz and 10 mm; (b) 1.5 Hz and 5 mm.*

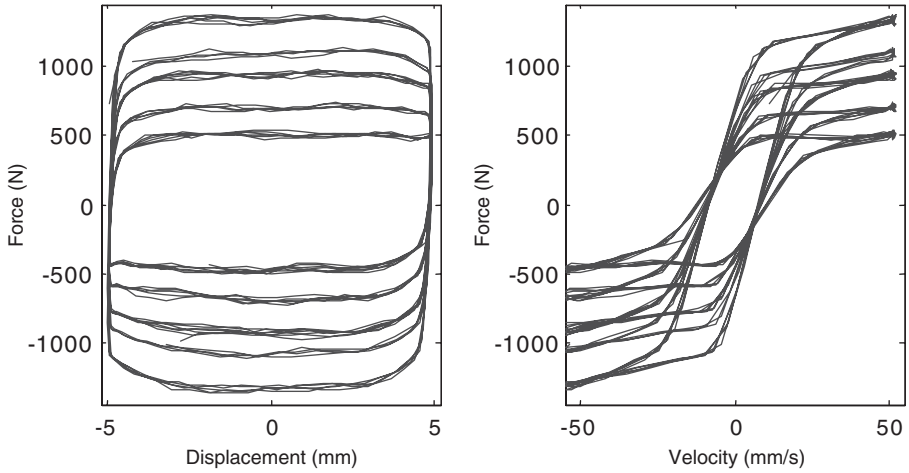

Figure A6. *The test data in excitation of 2 Hz and 5 mm.*

If there are 7 curves in a figure, the currents of the curves are 0, 0.5, 1, 1.5, 2, 2.5 and 3 A, respectively. If there are 5 curves in a figure, the currents for the curves are 0, 0.5, 1, 1.5 and 2A, respectively.

APPENDIX B: THE DETAILED PROCESS FOR THE THEORETICAL SOLUTION

Assuming the form of the first-order approximate solution is

$$x = \delta \sin(\omega t + \phi) \tag{B1}$$

Substituting Equation (B1) into Equation (31) and letting $\omega t + \phi = \pi/2$, one has

$$-m\omega^2\delta + k\delta + A_2\delta\omega \tan\theta_0 + A_1 \tanh(A_3\delta\omega \tan\theta_0) = p_0 \cos\phi \tag{B2}$$

From the view of energy conservation, the work done by excitation force is equal to the work done by damping force in a cycle, when the isolation system attains the steady motion. Then one has Equation (B3).

$$\oint (A_2(\dot{x} + \omega x \tan\theta_0) + A_1 \tan(A_3(\dot{x} + \omega x \tan\theta_0)))\dot{x}\,\mathrm{d}t = \oint (p_0 \sin\omega t)\dot{x}\,\mathrm{d}t \tag{B3}$$

The term $\tanh(A_3(\dot{x} + \omega x \tan\theta_0))$ is approximate to

$$\frac{A_3(\dot{x} + x\omega \tan\theta_0)}{\sqrt{1 + A_3^2(\dot{x} + x\omega \tan\theta_0)^2}}$$

Substituting it into the above equation, that is

$$\oint \left(A_2(\dot{x} + x\omega \tan\theta_0) + A_1 \frac{A_3(\dot{x} + x\omega \tan\theta_0)}{\sqrt{1 + A_3^2(\dot{x} + x\omega \tan\theta_0)^2}} \right) \dot{x}\,\mathrm{d}t = \oint \dot{x} p_0 \sin\omega t\,\mathrm{d}t \tag{B4}$$

Substituting Equation (B1) into Equation (B4) and integrating it, one can obtain

$$A_1 \cos\theta_0 g\left(\frac{A_3\delta\omega}{\cos\theta_0}\right) + A_2\delta\omega\pi = -p_0\pi \sin\phi \tag{B5}$$

where the function $g(\cdot)$ is defined by Equation (33).

Eliminating ϕ from Equations (B2) and (B5), one obtains Equation (32).

REFERENCES

Carlson, J.D., Catanzarite, D.M. and St. Clair, K.A. 1995. "Commercial Magnetorheological Fluid Devices," In: *Proceeding of the International Conference on Electro-Rheological, Magnetorheological Suspensions and Associated Technology*, Sheffield, England, UK, World Scientific Press, Rivers Edge, NJ, pp. 20–28.

Choi, S.-B. and Han, Y.-M. 2003. "MR Seat Suspension for Vibration Control of a Commercial Vehicle," *International Journal of Vehicle Design*, 31(2):202–215.

Choi, S.-B., Lee, S.-K. and Park, Y.-P. 2001. "A Hysteresis Model for Field-Dependent Damping Force of a Magnetorheological Damper," *Journal of Sound and Vibration*, 245(2):375–383.

Choi, Young-Tai, Wereley, Norman M. and Jeon, Young-Sik 2002. "Semi-active Vibration Isolation using Magnetorheological Isolators," In: *Proceedings of SPIE*, Vol. 4697, pp. 284–291.

Gandhi, Farhan, Wang, K.W. and Xia, Liba 2001. "Magneto-rheological Fluid Damper Feedback Linearization Control for Helicopter Rotor Application," *Smart Mater. Struc.*, 10(1):96–103.

Haijun, Xing, Jie, Ren and Wenwu, Guo 2002. "Experiment and Analysis of Properties of Magnetorheological Damper," *Journal of Shijiazhuang Railway Institute*, 15(3):33–35 (in Chinese).

Jolly, Mark R., Bender, Jonathan W. and Carlson Thomas, J. David 2000. "Properties and Application of Commercial Magnetorheological Fluids," Lord Research Center Lord Corporation, www.mrfuild.com.

Pang, Li, Kamath, Gopalakrishna, M. and Wereley, Norman, M. 1998. "Dynamic Characterization and Analysis of Magnetorheogical Dampers Behavior," *SPIE*, 3227:284–302.

Sims, N.D., Holmes, N.J. and Stanway, R. 2004. "A Unified Modeling and Model Updating Procedure for Electrorheological and Magnetorheological Vibration Dampers," *Smart Materials and Structures*, 13(1):100–121.

Spencer, Jr., B.F., Dyke, S.J., Sain, M.K. and Carlson, J.D. 1997. "Phenomenological Model of a Magnetorheological Damper," *Journal of Engineering Mechanics, ASCE*, 123(3):230–238.

Stanway, R., Sproston, J.L. and Stevens, N.G. 1987. "Non-linear Modeling of an Electrorheological Vibration Damper," *J. Electrostatics*, 20(2):167–184.

Stanway, R., Sproston, J.L. and El-Wahed, A.K. 1997. "Application of Electrorheological Fluids in Vibration Control: A Survey," *Smart Materials and Structures*, 5(3):351–358.

Wereley, N.M., Pang, L. and Kamath, G.M. 1998. "Idealized Hysteresis Modeling of Electrorheological and Magnetorheological Dampers," *Journal of Intelligent Material System and Structures*, 9:642–649.

Yang, Guangqiang 2001. "Large-scale Magnetorheological Fluid Damper for Vibration Mitigation: Modeling, Testing and Control," PhD Dissertation, Department of Civil Engineering and Geological Sciences, Nortre Dame, Indiana, December 2001.

Yang, S., Li, S., Wang, X., Gordaninejad, F. and Hitchcock, G. 2005. "A Hysteresis Model for Magneto-rheological Damper," *International Journal of Nonlinear Sciences and Numerical Simulation*, 6(2):139–144.